

Central Visual Function and Genotype–Phenotype Correlations in *PDE6A*-Associated Retinitis Pigmentosa

Laura Kuehlewein,^{1,2} Torsten Straßer,^{1,2} Gunnar Blumenstock,³ Katarina Stingl,¹ M. Dominik Fischer,² Barbara Wilhelm,⁴ Eberhart Zrenner,^{2,5} Bernd Wissinger,⁶ Susanne Kohl,⁶ Nicole Weisschuh,⁶ and Ditta Zobor^{2,7}; for the RD-CURE Consortium

¹University Eye Hospital, Centre for Ophthalmology, Eberhard Karls University of Tübingen, Tübingen, Germany

²Institute for Ophthalmic Research, Centre for Ophthalmology, Eberhard Karls University of Tübingen, Tübingen, Germany

³Department of Clinical Epidemiology, Eberhard Karls University of Tübingen, Tübingen, Germany

⁴STZ eyetrial at the Centre for Ophthalmology, Eberhard Karls University of Tübingen, Tübingen, Germany

⁵Werner Reichardt Centre for Integrative Neuroscience, Eberhard Karls University of Tübingen, Tübingen, Germany

⁶Molecular Genetics Laboratory, Institute for Ophthalmic Research, Centre for Ophthalmology, Eberhard Karls University of Tübingen, Tübingen, Germany

⁷Department of Ophthalmology, Semmelweis University, Budapest, Hungary

See the Appendix for the members of the RD-CURE Consortium.

Correspondence: Laura Kuehlewein, Centre for Ophthalmology, Eberhard Karls University of Tübingen, Elfriede-Aulhorn-Straße 7, 72076 Tübingen, Germany; laura.kuehlewein@med.uni-tuebingen.de.

LK and TS contributed equally to the work presented here and should therefore be regarded as equivalent authors.

Received: October 20, 2021

Accepted: April 14, 2022

Published: May 9, 2022

Citation: Kuehlewein L, Straßer T, Blumenstock G, et al. Central visual function and genotype–phenotype correlations in *PDE6A*-associated retinitis pigmentosa. *Invest Ophthalmol Vis Sci.* 2022;63(5):9. <https://doi.org/10.1167/iovs.63.5.9>

PURPOSE. Autosomal recessive retinitis pigmentosa (arRP) can be caused by mutations in the phosphodiesterase 6A (*PDE6A*) gene. Here, we describe the natural course of disease progression with respect to central retinal function (i.e., visual acuity, contrast sensitivity, and color vision) and establish a detailed genotype–phenotype correlation.

METHODS. Forty-four patients (26 females; mean age \pm SD, 43 \pm 13 years) with a confirmed genetic diagnosis of *PDE6A*-associated arRP underwent comprehensive ophthalmological examinations including best-corrected visual acuity (BCVA) with Early Treatment Diabetic Retinopathy Study charts, contrast sensitivity (CS) with Pelli–Robson charts at distances of 3 m and 1 m, and color vision testing using Roth 28-Hue and Panel D-15 saturated color cups.

RESULTS. The most frequently observed variants were c.998+1G>A/p.?, c.304C>A/p.R102S, and c.2053G>A/p.V685M. Central retinal function in patients homozygous for variant c.304C>A/p.R102S was better when compared to patients homozygous for variant c.998+1G>A/p.?, although the former were older at baseline. Central retinal function was similar in patients homozygous for variant c.304C>A/p.R102S and patients heterozygous for variants c.304C>A/p.R102S and c.2053G>A/p.V685M, although the latter were younger at baseline. Annual decline rates in central retinal function were small.

CONCLUSIONS. We conclude that the severity of the different disease-causing *PDE6A* mutations in humans with respect to central visual function may be ranked as follows: c.2053G>A/p.V685M in homozygous state (most severe) > c.998+1G>A/p.? in homozygous state > c.304C>A/p.R102S and c.2053G>A/p.V685M in compound-heterozygous state > c.304C>A/p.R102S in homozygous state (mildest). The assessment of treatment efficacy in interventional trials will remain challenging due to small annual decline rates in central retinal function.

Keywords: retinitis pigmentosa, phosphodiesterase, gene therapy

Retinitis pigmentosa (RP) is a clinically and genetically heterogeneous group of inherited retinal disorders (IRDs) and is one of the most common types of retinal degenerations worldwide with a prevalence of 1/4000.¹ So far, several dozens of genes have been associated with RP, defects in which cause a progressive loss of rod photoreceptor function, followed and accompanied by cone photoreceptor dysfunction.² Although the pathophysiological origin can vary depending on the disease-causing genetic defect, RP clinically manifests with early-onset night blindness, followed by daytime visual field defects progressing from the mid-periphery to the periphery and the center. Best-

corrected visual acuity (BCVA) typically remains relatively preserved until macular involvement by macular edema and/or photoreceptor atrophy causes additional central vision loss.³

Mutations in the phosphodiesterase 6A (*PDE6A*) gene (OMIM *180071, #613810) were first reported to cause autosomal recessive RP (arRP) in humans in 1995.^{4,5} The *PDE6A* gene encodes the alpha subunit of the cyclic guanosine monophosphate (cGMP) phosphodiesterase, which plays a central role in the rod phototransduction cascade.⁶ Dysfunction or loss of the *PDE6A* protein leads to defective biochemical signaling of light stimuli and dysregulation of cGMP in

rod photoreceptor outer segments, triggering cell death in rods and secondarily in cones.

In recent years, important advances have been made in the development of treatments that aim to slow or stop disease progression or even to restore some visual function in patients with IRDs. However, an imbalance exists between the rapid advances in therapy development and the available knowledge on the clinical disease course and the phenotypic spectrum for each specific gene of interest.⁷ Prospective observational studies are rare in these often relatively small patient populations. *PDE6A* is one of several candidate genes currently under investigation. In 2012, the RD-Cure Consortium was established as a collaborative project for the clinical translation of gene therapy for patients with *PDE6A*-associated arRP. Homologous animal models including a dog model with a frameshift truncating mutation (p.N616Tfs*39) and three mouse models with missense mutations (p.V685M, p.D562W, and p.D670G) have been studied, all showing a range of phenotype severities, and proof-of-concept supplemental gene therapy was demonstrated in these animal models.^{8–16} Parallel to preclinical experiments and vector development, a prospective longitudinal study on the clinical features and genetic findings of patients with *PDE6A*-associated arRP was initiated to precisely characterize the natural course of the disease.⁸

Previous studies have reported a prevalence of *PDE6A* mutations in about 3% to 4% of arRP patients in North America, in about 2% of cases in cohorts of French and Pakistani patients, and in about 1% of families with IRDs in Israel.^{17–20} Our *PDE6A*-RP patient cohort indicates a frequency of *PDE6A*-associated arRP of 1.6% in Germany and shows a highly heterogeneous disease course depending on the genotype. To further investigate disease characteristics, we focus here on the natural course of disease progression with respect to central retinal function (i.e., visual acuity, contrast sensitivity, and color vision). These are crucial in determining patient eligibility criteria and clinical endpoints in ongoing and future clinical trials to assess the safety and efficacy of novel treatments.

METHODS

This prospective longitudinal observational cohort study (ClinicalTrials.gov NCT02759952) was conducted in accordance with the tenets of the Declaration of Helsinki with approval from the ethics committee of the University of Tübingen, Tübingen, Germany. Written informed consent was obtained from all patients. Patients were recruited from the Clinics for Inherited Retinal Degenerations at the Centre for Ophthalmology of the University of Tübingen and from 12 collaborating European referral centers. All patients were examined at the Centre for Ophthalmology of the University of Tübingen. The patients enrolled in this study had a confirmed genetic diagnosis of *PDE6A*-associated arRP as previously described.⁸ Of the 57 patients included in our initial patient cohort, 44 underwent more detailed testing and were included in this analysis. Subgroup analyses were performed for the most common variants observed in this cohort. Outcome variables were tested for both eyes of each subject at each visit, but without fixed intervals between visits. Patients were included in this study from 10 European countries, requiring significant efforts for traveling, which hampered evenly spaced intervals between visits. Ten of the 44 patients (23%) were lost to follow-up after the first visit.

Ophthalmological Examinations

Comprehensive ophthalmological examinations were performed in all patients, including BCVA as determined by Early Treatment Diabetic Retinopathy Study (ETDRS) charts, contrast sensitivity (CS) with Pelli–Robson charts at distances of 3 m and 1 m, and color vision testing using Roth 28-Hue and Panel D-15 saturated color cups. To determine BCVA, the ETDRS charts (Lighthouse Low Vision Products, New York, NY, USA) were viewed at a distance of 4 m for both eyes independently with optimal optical correction. If the patient read less than 20 letters at 4 m, the chart was moved from 4 m to 1 m with an additional +0.75 diopter (D) lens in the frame to account for the distance. If the patient was unable to read letters correctly at both distances, the patient was tested for count fingers (CF), hand movement (HM), and light perception (LP) or no light perception, recording the distance at which CF, HM, or LP was seen. BCVA was converted to logMAR visual acuity for statistical analysis.²¹ CS was determined with Pelli–Robson contrast sensitivity charts (Metropia Ltd., Harlow, UK) viewed at distances of 3 m and 1 m for both eyes independently with optimal optical correction. The test was stopped when the patient failed to identify two of the three letters in a triplet correctly, despite encouraging the patient to read or guess. CS was then recorded as logCS units.

Color vision was determined with color cups (Roth 28-Hue and/or Panel D-15 saturated) viewed at reading distance on a table illuminated with constant cold lighting (270 lux) for both eyes independently with optimal optical correction. The color cups were put on the table in a randomly mixed group with the colors facing up. The patient was instructed to select the cups most closely matching in chromaticity and arrange them in a row. The sequence of the numbers on the back of the cups was recorded. The total error score (TES) and color confusion index (CCI) were calculated for Roth 28-Hue and Panel D-15 color vision testing, respectively.^{22–25}

Statistical Analysis

Statistical analyses were carried out using SPSS Statistics for Windows (IBM, Chicago, IL, USA) and JMP (SAS Institute, Cary, NC, USA). Random effects models, fit by restricted maximum likelihood estimates, were used for best unbiased linear prediction (BLUP) of the progression per year of age of the dependent variables (*Y*) (BCVA, CS at 3-m distance, CS at 1-m distance, Roth TES, and Panel CCI).²⁶ To account for the repeated measures, the examined eye (right eye, OD; left eye, OS) nested in participant and genetics and participant nested in genetics were included as additional random effects (Equation 1):

$$Y_{ijk} = \mu + age + genetics_i + participant_{j(i)} + eye_{k(i,j)} + \varepsilon_{ijk} \quad (1)$$

Prior to utilizing the results of the models, the normal distribution of the conditional model residuals was confirmed visually. The homoscedasticity of the variances was assessed using the Brown–Forsythe test and reported in case of violations of the assumptions.²⁷

RESULTS

Of the 44 patients included in this study, 59% (26/44) were female. Mean age \pm SD at baseline was 43 ± 13 years (range, 18–78). Information on the onset of disease and

disease duration was collected from all patients at the first or subsequent visits. Statistical analyses were performed with disease duration *or* the age of the patient at the respective visit and yielded the same results. Disease onset was defined as the first symptom noticed by the patient or parents, and this was usually night blindness from birth or during early childhood. We believe that, if the patient reported first symptoms during his or her first decade of life in particular, the variable “disease duration” would give rise to estimated rather than precise numbers. In our study, 33 of the 44 patients (75%) reported first symptoms during their first decade of life. Given these findings, we decided to report only values calculated with the age at the visit rather than disease onset or disease duration.

Genetic Results

Variants were classified according to their pathogenicity based on American College of Medical Genetics and Genomics guidelines.^{8,28} All 44 patients harbored potentially disease-causing variants compatible with autosomal recessive *PDE6A*-associated arRP (Table 1). Fifty-nine percent (26/44) were homozygous for disease-causing variants, and 41% (18/44) were heterozygous for two different *PDE6A* variants each. Biallelism was validated in 59% cases (26/44). The mutation spectrum was comprised of 25 unique variants (Fig. 1). The most frequently observed variants were c.998+1G>A/p.? (14 alleles, homozygous in seven patients), c.304C>A/p.R102S (17 alleles, homozygous in five patients), and c.2053G>A/p.V685M

TABLE 1. General, Genetic, and Ophthalmological Characteristics of Patients with *PDE6A*-Associated arRP at Baseline

ID	Gender	Age (y)	Variant 1	Variant 2	BCVA (logMAR)	
					OD	OS
23	F	29	c.998+1G>A/p.?	c.998+1G>A/p.?	0.60	0.00
8	M	33	c.998+1G>A/p.?	c.998+1G>A/p.?	0.10	0.10
25	F	35	c.998+1G>A/p.?	c.998+1G>A/p.?	1.00	1.00
26	F	37	c.998+1G>A/p.?	c.998+1G>A/p.?	0.30	0.20
12	F	42	c.998+1G>A/p.?	c.998+1G>A/p.?	0.20	0.20
22	M	46	c.998+1G>A/p.?	c.998+1G>A/p.?	0.70	0.90
24	F	47	c.998+1G>A/p.?	c.998+1G>A/p.?	1.00	0.70
27	F	37	c.304C>A/p.R102S	c.304C>A/p.R102S	0.20	0.20
34	M	40	c.304C>A/p.R102S	c.304C>A/p.R102S	-0.10	0.00
47	M	44	c.304C>A/p.R102S	c.304C>A/p.R102S	0.10	0.10
7	F	50	c.304C>A/p.R102S	c.304C>A/p.R102S	0.20	0.50
1	F	78	c.304C>A/p.R102S	c.304C>A/p.R102S	1.00	0.30
49	M	26	c.304C>A/p.R102S	c.2053G>A/p.V685M	0.00	0.00
30	F	29	c.304C>A/p.R102S	c.2053G>A/p.V685M	0.30	0.20
29	F	37	c.304C>A/p.R102S	c.2053G>A/p.V685M	0.20	0.10
15	M	37	c.304C>A/p.R102S	c.2053G>A/p.V685M	0.20	0.20
16	M	49	c.304C>A/p.R102S	c.2053G>A/p.V685M	0.10	0.20
10	F	45	c.2053G>A/p.V685M	c.2053G>A/p.V685M	1.20	1.00
11	M	46	c.2053G>A/p.V685M	c.2053G>A/p.V685M	0.70	0.90
50	F	18	c.1957C>T/p.R653*	c.998+2T>G/p.?	0.00	0.00
5	F	22	c.769C>T/p.R257*	c.769C>T/p.R257*	0.30	0.30
4	F	23	c.769C>T/p.R257*	c.769C>T/p.R257*	0.40	0.30
17	M	23	c.769C>T/p.R257*	c.769C>T/p.R257*	0.00	0.00
20	F	33	c.1957C>T/p.R653*	c.1957C>T/p.R653*	0.50	0.40
6	M	33	c.1620+1G>A/p.?	c.1705C>A/p.Q569K	0.00	0.10
36	F	34	c.1705C>A/p.Q569K	c.1705C>A/p.Q569K	0.00	0.00
48	F	35	c.1683G>A/p.W561*	c.1263+1G>A/p.?	0.10	0.00
21	M	37	c.1957C>T/p.R653*	c.1957C>T/p.R653*	0.20	0.20
2	F	38	c.63_68del/p.K21_Y23delinsN	c.1926+1G>A/p.?	0.30	0.70
28	M	38	c.305G>A/p.R102H	c.305G>A/p.R102H	0.20	0.50
3	M	40	c.304C>A/p.R102S	c.1689C>A/p.H563Q	0.00	0.10
14	F	42	c.1862T>G/p.L621R	c.2053G>A/p.V685M	0.10	0.10
35	F	42	c.84C>G/p.Y28*	c.84C>G/p.Y28*	1.20	1.20
19	M	43	c.1957C>T/p.R653*	c.2332_2335del/p.D778Lfs*42	0.30	0.30
46	M	49	c.304C>A/p.R102S	c.1705C>A/p.Q569K	0.20	0.10
44	F	53	c.627+2T>G/p.?	c.627+2T>G/p.?	0.50	0.80
41	F	55	c.612del/p.K205Rfs*16	c.612del/p.K205Rfs*16	0.50	0.20
18	M	55	c.1235T>C/p.F412S	c.1966G>T/p.E656*	1.50	2.30
31	M	56	c.1705C>A/p.Q569K	c.1065+2T>A/p.?	0.50	0.50
33	F	60	c.1705C>A/p.Q569K	c.1065+2T>A/p.?	0.60	0.20
38	F	62	c.1705C>A/p.Q569K	c.1705C>A/p.Q569K	2.30	2.30
39	M	63	c.1957C>T/p.R653*	c.1956_1957ins20/p.R653*	0.30	0.30
45	F	65	c.959A>G/p.D320G	c.1749C>G/p.Y583*	0.40	0.30
32	F	66	c.1705C>A/p.Q569K	c.1065+2T>A/p.?	1.10	1.10

Patients are sorted by their genetic background and age at baseline. F, female; M, male.

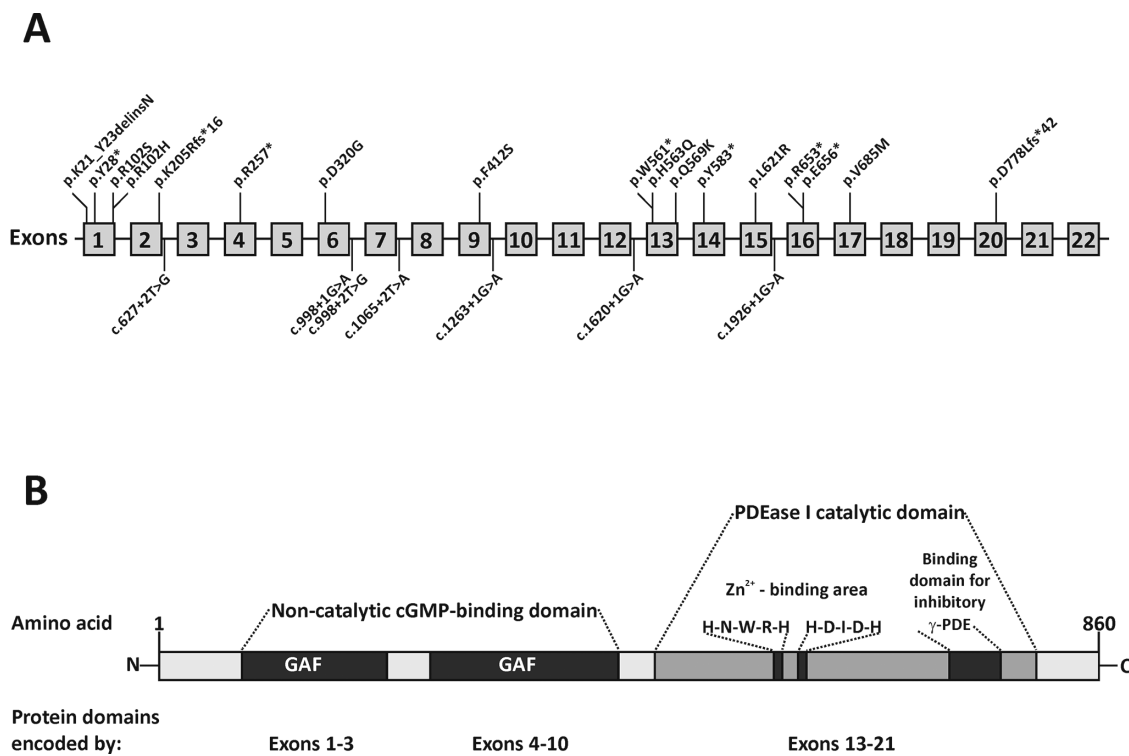


FIGURE 1. Variant distribution. (A) The 22 exons of *PDE6A* (NM_000440.3) are represented by *gray boxes*. Note that exons and the intervening intronic sequences (represented by *black horizontal lines*) are not drawn to scale. Each variant identified in our cohort is shown above the respective exon (for missense, nonsense, and indel variants) or below the respective intron (for splice site variants). (B) Protein structure with the non-catalytic cGMP-binding domain and the PDEase I catalytic domain.

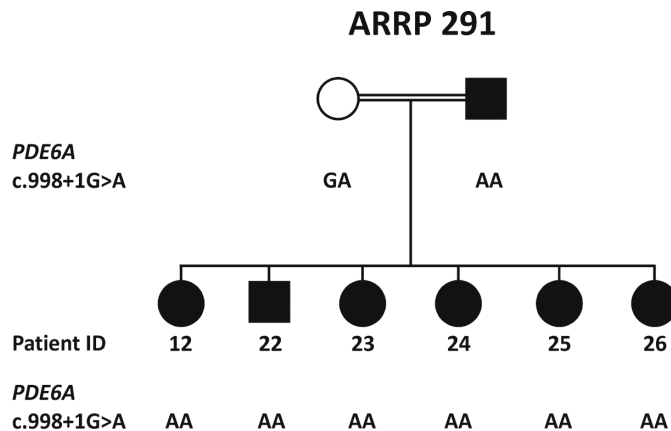


FIGURE 2. Pedigree of family ARR 291 carrying variant c.998+1G>A/p.? homozygously. *Circles* indicate female family members, *squares* indicate male family members. Affected family members are indicated by *black symbols*. Note that the father of the six siblings also carries the respective variant homozygously. Also note the consanguinity in the parents.

(10 alleles, homozygous in two patients). Five patients carried the c.304C>A/p.R102S and c.2053G>A/p.V685M variants, each heterozygously (Table 1). In these, compound heterozygosity was confirmed in all cases except one (case number 49). Of note, the high number of c.998+1G>A/p.? alleles in this study related to the fact that six siblings from the same family carried this variant homozygously. The pedigree of this family is provided in Figure 2.

Clinical Results

Symmetry Between Eyes and Correlation Between Modalities. Baseline data are shown in Table 2. BCVA symmetry between right and left eyes at baseline was high ($r = 0.89$; $P < 0.01$; $n = 44$). The difference in BCVA between right and left eyes was 0.2 logMAR and greater in 11 of the 44 patients (25%). All of these 11

TABLE 2. Baseline Findings of Patients with *PDE6A*-Associated arRP

Eye	OD		OS	
	n	Median (Range)	n	Median (Range)
BCVA (logMAR)	44	0.3 (–0.1 to 2.30)	44	0.2 (0–2.30)
logCS at 3 m distance	36	1.50 (0–2.0)	40	1.35 (0–2.0)
logCS at 1 m distance	39	1.50 (0–2.0)	39	1.50 (0–2.0)
Roth TES	33	24 (0–732)	32	42 (0–744)
Panel CCI	36	1.16 (1.0–3.0)	37	1.12 (1–4)

patients exhibited additional and asymmetrical macular pathology: cystoid macular edema (three patients), epiretinal membrane with or without traction (four patients), macular hole (one patient), and atrophy (three patients). CS symmetry between right and left eyes at baseline was calculated as $r = 0.75$ ($P < 0.01$; $n = 36$) at 3-m distance and $r = 0.83$ ($P < 0.01$; $n = 39$) at 1-m distance. Color vision symmetry between right and left eyes at baseline was calculated as $r = 0.85$ ($P < 0.01$; $n = 31$) for Roth TES and $r = 0.83$ ($P < 0.01$; $n = 36$) for Panel CCI.

Correlation was strong between BCVA and CS at the 3-m distance ($r = -0.87$; $P < 0.01$; $n = 76$ measurements) and BCVA and CS at the 1-m distance ($r = -0.85$; $P < 0.01$; $n = 78$ measurements). Similarly, correlation was strong between BCVA and Roth TES ($r = 0.72$; $P < 0.01$; $n = 65$ measurements) and BCVA and Panel CCI ($r = 0.75$; $P < 0.01$; $n = 73$ measurements). The correlation between CS at 3-m distance and CS at 1-m distance and the correlation between Roth TES and Panel CCI are shown in Figure 3.

Genotype–Phenotype Correlations. We analyzed subgroups according to the results of their genetic analysis: group 1, patients homozygous for variant c.998+1G>A/p.? ($n = 7$); group 2, patients homozygous for variant c.304C>A/p.R102S ($n = 5$); and group 3, patients heterozygous for variants c.304C>A/p.R102S and c.2053G>A/p.V685M ($n = 5$). Only two siblings carried the variant c.2053G>A/p.V685M homozygously. Baseline findings of all groups are shown in Figure 4. Central retinal function in group 2 was better when compared to group 1, although patients were older at baseline. Central retinal

function was similar in groups 2 and 3, although patients in group 3 were younger at baseline. The two siblings homozygous for variant c.2053G>A/p.V685M (ages 45 and 46 years, respectively) showed markedly reduced visual function at baseline (BCVA of 1.2/1.0 and 0.7/0.9 logMAR in their right and left eyes, respectively).

Progression. Mean duration \pm SD between baseline and last follow-up was 28 ± 12 months. Median follow-up between visits was 27 months (range, 9–53). The residuals of both statistical models (see above) for color vision (Roth TES and Panel CCI) did not follow a normal distribution and were heteroscedastic: Brown–Forsythe Roth TES, $F(1, 149) = 53.84$, $P < 0.01$; Panel CCI, $F(1, 170) = 86.77$, $P < 0.01$. The other models satisfied the assumptions for normality and homoscedasticity of residuals. Progression rates are provided in Table 3 and shown in Figure 5.

DISCUSSION

PDE6A-associated arRP is a primary rod disease, leading to typical rod–cone dystrophy presenting with night blindness and progressive visual field loss, but with relatively preserved central vision during the course of the disease. Previously, we reported on the largest patient cohort with arRP associated with variants in the *PDE6A* gene, showing a range of phenotypic severities but overall mild to moderate disease characteristics.⁸

Central retinal function is an important clinical endpoint in current phase I/II interventional trials targeting photoreceptors in RP, such as gene therapy trials for RP associated with variants in *RHO* (ClinicalTrials.gov identifier NCT 04123626), *MERTK* (NCT 01482195), *PDE6B* (NCT 03328130), and *RPGR* (NCT 03316560).^{7,12,29} In this work, we assessed central retinal function in *PDE6A*-associated arRP (BCVA, CS, and color vision) and their decline rates during the natural course of the disease.

We observed an excellent intra-individual symmetry in all tested modalities, but most so in BCVA. Differences in BCVA of >0.2 logMAR were found in only a few cases and were caused by various macular pathologies that were present or more pronounced in one eye when compared to the other eye. The high degree of symmetry is highly relevant for any

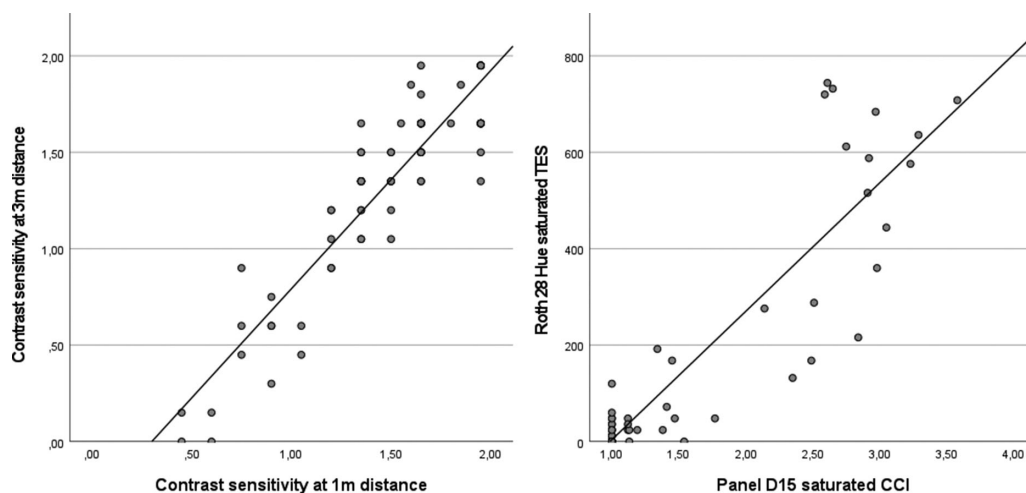


FIGURE 3. Correlation between contrast sensitivity at distances of 3 m and 1 m ($r = 0.91$; $P < 0.01$; $n = 71$ measurements) and between Roth 28-Hue and Panel D-15 saturated tests ($r = 0.90$; $P < 0.01$; $n = 61$ measurements) in *PDE6A*-associated arRP. Note the ceiling effect in Panel D-15 saturated color vision testing.

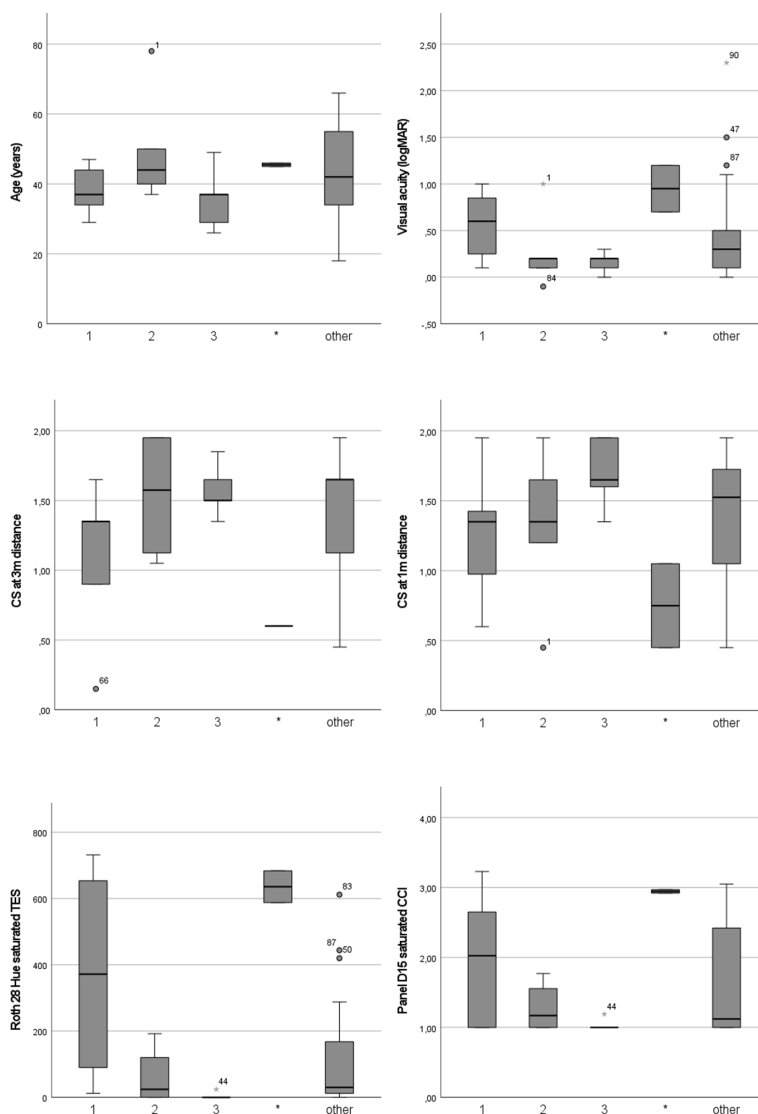


FIGURE 4. Genotype-associated age, visual acuity, contrast sensitivity, and color vision in *PDE6A*-associated arRP. Baseline findings of right eyes. Group 1 was comprised of patients homozygous for variant c.998+1G>A/p.? ($n = 7$); group 2, patients homozygous for variant p.R102S ($n = 5$); and group 3, patients heterozygous for variants c.304C>A/p.R102S and c.2053G>A/p.V685M ($n = 5$). The two siblings carrying the variant c.2053G>A/p.V685M homozygously are indicated with a *black asterisk*. The remaining patients are sub-summarized by “other.” Note that the central retinal function in group 2 was better when compared to group 1, although patients were older at baseline. Also note that central retinal function was similar in groups 2 and 3, although patients in group 3 were younger at baseline.

TABLE 3 Progression Rates for Visual Acuity, Contrast Sensitivity, and Color Vision Findings of Patients with *PDE6A*-Associated arRP

Modality	n	Progression Per Year		Parameter Estimates	
		BLUP	95% Confidence Interval	t-Statistic	P
BCVA (logMAR)	208	0.015	(0.007–0.023)	$t(82.78) = 3.95$	<0.01
logCS at 3-m distance	194	−0.02	(−0.03 to −0.01)	$t(56.54) = −3.52$	<0.01
logCS at 1-m distance	184	−0.02	(−0.03 to −0.01)	$t(53.30) = −4.64$	<0.01
Roth TES	151	11.23	(6.25–16.21)	$t(40.74) = 4.55$	<0.01
Panel CCI	172	0.020	(0.002–0.039)	$t(21.85) = 2.27$	0.03

interventional trial treating patients with novel treatments such as gene therapy, as the second eye will usually be chosen as a control.

As expected, CS at a distance of 3 m strongly correlated with CS at a distance of 1 m, as did color vision tested with

the Roth 28-Hue and Panel D-15 tests in our sample of visually impaired patients. The correlation between BCVA and CS was stronger than the correlation between BCVA and color vision testing. Annual decline rates were 0.015 log units for BCVA and 0.02 log units for CS at distances of 3 m

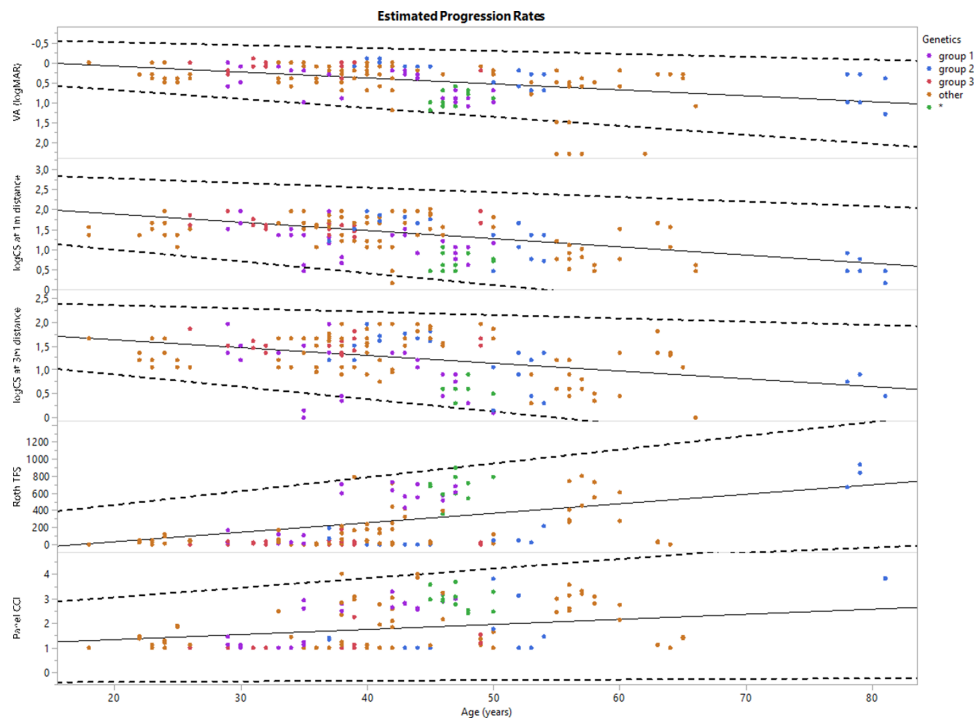


FIGURE 5. Estimated progression rates in visual acuity, contrast sensitivity, and color vision in *PDE6A*-associated arRP. The *dashed lines* indicate the 95% confidence intervals.

and 1 m. The progression rates determined for color vision testing (Roth TES and Panel CCI) should be regarded with caution, as the models failed the assumptions of normality and homoscedasticity of residuals, resulting in a possible overestimation of the statistical significance of the reported values. Annual decline rates of 0.015 and 0.02 logMAR (i.e., as seen for BCVA and CS in this study) are small, given that a change in BCVA is usually considered clinically meaningful when exceeding 15 letters (i.e., 0.1 logMAR).^{30–32} A progression rate of 0.037 log units has been reported for a different cohort of patients with *PDE6A*-associated arRP.¹⁷ Other studies have reported annual decline rates of 1%, 2%, and 8.6% for RP overall.^{33–36} The small estimated progression rates suggest, on one hand, a slow disease course favorable for patients but, on the other hand, clearly limit BCVA changes as useful endpoints in treatment trials that aim at slowing down disease progression. A minimum difference of 15 letters between treated and control eyes would require an observational study to last 15 years. Similar observations concerning the non-suitability of BCVA as endpoint in clinical trials were made in the PROGSTAR study, which calculated that 22 years of observation would be required to reach the necessary difference between treated and untreated eyes in patients with Stargardt disease.³⁷

The model implied in this study to calculate progression rates included genetics as a random effect. We found no statistically significant effect on the progression rate with respect to the genotype of the patient. Moreover, interindividual differences were found to have a larger effect on the progression rate than the age of the patient. We thus decided to report mean progression rates including the whole cohort.

At the genetic level, several recurrent variants were observed in our cohort: c.304C>A/p.R102S (17 of 88 mutant alleles in the cohort), c.998+1G>A/p.? (14 of 88 mutant alleles in the cohort), and c.2053G>A/p.V685M

(10 of 88 mutant alleles in the cohort). Note that the high frequency of variant c.998+1G>A/p.? in this study relates to the fact that six siblings from the same family carried this variant homozygously. Our clinical findings revealed a remarkable genotype–phenotype correlation: Although variant c.304C>A/p.R102S was associated with milder disease, variants c.998+1G>A/p.? and c.2053G>A/p.V685M led to a more severe phenotype. This held true for central retinal function, as patients homozygous for variant c.304C>A/p.R102S (group 2) had better central retinal function, but patients homozygous for either c.998+1G>A/p.? (group 1) or c.2053G>A/p.V685M showed worse central retinal function. Patients heterozygous for variants c.304C>A/p.R102S and c.2053G>A/p.V685M (group 3) had worse central retinal function when compared to group 2, indicating a negative contribution of the second variant (c.2053G>A/p.V685M) to the phenotype of the patients.

Given this detailed analysis and previously published clinical findings,⁸ we argue that the severity of the different disease-causing *PDE6A* mutations in humans may be ranked as follows: c.2053G>A/p.V685M in homozygous state (most severe) > c.998+1G>A/p.? in homozygous state > c.304C>A/p.R102S and c.2053G>A/p.V685M in compound-heterozygous state > c.304C>A/p.R102S in homozygous state (mildest).⁸ Our results are comparable to the clinical findings reported by Khateb et al.¹⁷; however, note that the two patient cohorts showed differences in their genotypic composition. In the latter study, only four of the patients harbored the milder variant c.304C>A/p.R102S (one patient homozygously), whereas only one of the patients was heterozygous for c.998+1G>A/p.?, and no patients were included with variant c.2053G>A/p.V685M.¹⁷

Our clinical findings are in line with biochemical and preclinical observations. Both variants, c.304C>A/p.R102S and c.998+1G>A/p.?, affect the non-catalytic cGMP-binding

domain of the PDE6A protein; however, c.998+1G>A/p.? is considered a *null* allele, in contrast to the missense variant c.304C>A/p.R102S. The missense variant c.2053G>A/p.V685M affects the catalytic domain of PDE6A. A valine residue at position 685 is completely conserved across species for alpha- and beta-catalytic subunits, suggesting an important and specific role in the catalytic function of the PDE6 complex.^{20,38} Sothilingam et al.¹⁶ performed a detailed analysis of several *Pde6a* missense variants in mouse models (namely, p.V685M, p.R562W, and p.D670G), which confirmed the severity of different *Pde6a* variants and indicated that compound heterozygous mutant mice (p.V685M/p.R562W) show an intermediate phenotype when compared to the respective homozygous mutants. Specifically, the severity of the four different *PDE6A* genotypes could be ranked by the pace of photoreceptor degeneration: p.V685M homozygous (fastest) > p.V685M;p.R562W > p.R562W homozygous > p.D670G homozygous (slowest). Note that the p.V685M variant in the mouse mutant is homologous to the c.2053G>A/p.V685M variant in human patients.

Results of this detailed analysis on central retinal function in patients with *PDE6A*-RP show remarkable and strong association with the respective genetic variants within this cohort. Such a correlation is rarely described and may help in determining whether a patient is eligible to participate in interventional trials. Given that PDE6A is rod specific, ideally, endpoints for treatment trials will include measures of rod function (e.g., dark-adapted chromatic perimetry, pupil campimetry). Yet, safety and efficacy measures in clinical trials still focus on cone-derived measures, as the benefit for the patient in daily life unequivocally rests on a well-functioning cone system, especially in the central retina. Nevertheless, treatment of rods in some forms of IRD seems crucial, as cones rely on rods to maintain their metabolism.³⁹ Therefore, assessing and interpreting central retinal function in RP is highly important. Anatomical endpoints such as ellipsoid zone width on optical coherence tomography imaging may also be useful in future clinical trials. The same applies to microperimetry, especially at the border zones of functioning retina. The criterion for microperimetry concerning responders to therapy, accepted by the U.S. Food and Drug Administration, is a demonstration of improvement in sensitivity of at least 7 dB in at least five testing locations in the centermost 36 points of a 10-2 grid.⁴⁰ This criterion may be applicable to *PDE6A*-RP, as well. The results of our study also point out disease-specific limitations. Annual decline rates in central retinal function are small; therefore, interpretation of treatment safety and efficacy remains challenging. Finally, our study will help clinicians in counseling their patients.

Acknowledgments

The authors sincerely thank their collaborators: **Sten Andreasson** (Department of Ophthalmology, Skåne University Hospital, Lund University, Lund, Sweden); **Carmen Ayuso** (Department of Genetics, IIS-Fundación Jiménez Díaz University Hospital, Universidad Autónoma de Madrid [IIS-FJD, UAM], and Centre for Biomedical Research on Rare Diseases, Madrid, Spain); **Sandro Banfi** (Telethon Institute of Genetics and Medicine–Pozzuoli [NA] and Medical Genetics, Department of Precision Medicine, University of Campania “Luigi Vanvitelli,” Naples, Italy); **Antje Bernd**, **Dominik Fischer**, and **Katarina Stingl** (University Eye Hospital, Centre for Ophthalmology, Eberhard Karls University of Tübingen, Tübingen, Germany); **Beatrice Bocquet** and

Isabelle Meunier (Institute for Neurosciences of Montpellier U1051, University of Montpellier, and National Center for Rare Diseases, Genetics of Sensory Diseases, University Hospital, Montpellier, France); **Camiel J.F. Boon** (Department of Ophthalmology, Leiden University Medical Center, Leiden University, Leiden, the Netherlands, and Department of Ophthalmology, Amsterdam University Medical Centers, Amsterdam, the Netherlands); **Susan Downes** (Nuffield Laboratory of Ophthalmology, Nuffield Department of Clinical Neuroscience, University of Oxford, Oxford, UK); **Frank G. Holz** (Department of Ophthalmology, University of Bonn, Bonn, Germany); **Ulrich Kellner** (Rare Retinal Disease Center, Augenzentrum Siegburg, MVZ Augenärztliches Diagnostik und Therapiezentrum GmbH and RetinaScience, Bonn, Germany); **Bart P. Leroy** (Department of Ophthalmology, Ghent University Hospital, Ghent, Belgium; Center for Medical Genetics, Ghent University Hospital, Ghent, Belgium; Division of Ophthalmology, Children’s Hospital of Philadelphia, Philadelphia, PA, USA; and Center for Cellular and Molecular Therapeutics, Children’s Hospital of Philadelphia, Philadelphia, PA, USA); **Fadi Nasser** (Institute for Ophthalmic Research, Centre for Ophthalmology, Eberhard Karls University of Tübingen, Tübingen, Germany); **Thomas Rosenberg** (Department of Ophthalmology, Kennedy Center, Rigshospitalet, Copenhagen, Denmark); **Günther Rudolph** (Ophthalmogenetik, Augenklinik, Klinikum der Universität München, Munich, Germany); **Alberta A.H.J. Thiadens** (Department of Ophthalmology, Erasmus MC, Rotterdam, the Netherlands).

Supported by funds from the Tistou and Charlotte Kerstan Foundation.

Disclosure: **L. Kuehlewein**, Novartis (F); **T. Straßer**, None; **G. Blumenstock**, None; **K. Stingl**, ProQR (C, F), ViGeneron (C), Novartis (C, H), SANTEN (C), Nayan Therapeutics (C), Johnson & Johnson (F) with all payments to the Center for Ophthalmology, University of Tuebingen to support research; **M.D. Fischer**, Fischer Consulting Limited (F); **B. Wilhelm**, None; **E. Zrenner**, None; **B. Wissinger**, None; **S. Kohl**, None; **N. Weisschuh**, None; **D. Zobor**, None

References

1. Pagon RA. Retinitis pigmentosa. *Surv Ophthalmol*. 1988;33(3):137–177.
2. Retinal Information Network. RetNet: Retinal Information Network. Available at: <https://sph.uth.edu/RETNET/>. Accessed April 28, 2022.
3. Tsang SH, Sharma T. Retinitis pigmentosa (non-syndromic). *Adv Exp Med Biol*. 2018;1085:125–130.
4. Dryja TP, Finn JT, Peng YW, McGee TL, Berson EL, Yau KW. Mutations in the gene encoding the alpha subunit of the rod cGMP-gated channel in autosomal recessive retinitis pigmentosa. *Proc Natl Acad Sci USA*. 1995;92(22):10177–10181.
5. Huang SH, Pittler SJ, Huang X, Oliveira L, Berson EL, Dryja TP. Autosomal recessive retinitis pigmentosa caused by mutations in the alpha subunit of rod cGMP phosphodiesterase. *Nat Genet*. 1995;11(4):468–471.
6. Zhang X, Cote RH. cGMP signaling in vertebrate retinal photoreceptor cells. *Front Biosci*. 2005;10:1191–1204.
7. Talib M, Boon CJF. Retinal dystrophies and the road to treatment: clinical requirements and considerations. *Asia Pac J Ophthalmol (Phila)*. 2020;9(3):159–179.
8. Kuehlewein L, Zobor D, Andreasson SO, et al. Clinical phenotype and course of PDE6A-associated retinitis pigmentosa disease, characterized in preparation for a gene supplementation trial. *JAMA Ophthalmol*. 2020;138(12):1241–1250.

9. Mowat FM, Occelli LM, Bartoe JT, et al. Gene therapy in a large animal model of PDE6A-retinitis pigmentosa. *Front Neurosci.* 2017;11:342.
10. Occelli LM, Schön C, Seeliger MW, Biel M, Michalakakis S, Petersen-Jones SM. Gene supplementation rescues rod function and preserves photoreceptor and retinal morphology in dogs, leading the way toward treating human PDE6A-retinitis pigmentosa. *Hum Gene Ther.* 2017;28(12):1189–1201.
11. Pasmanter N, Occelli LM, Petersen-Jones SM. ERG assessment of altered retinal function in canine models of retinitis pigmentosa and monitoring of response to translatable gene augmentation therapy. *Doc Ophthalmol.* 2021;143(2):171–184.
12. Petersen-Jones SM, Occelli LM, Biel M, Michalakakis S. Advancing gene therapy for PDE6A retinitis pigmentosa. *Adv Exp Med Biol.* 2019;1185:103–107.
13. Sakamoto K, McCluskey M, Wensel TG, Naggert JK, Nishina PM. New mouse models for recessive retinitis pigmentosa caused by mutations in the *Pde6a* gene. *Hum Mol Genet.* 2009;18(1):178–192.
14. Tuntivanich N, Pittler SJ, Fischer AJ, et al. Characterization of a canine model of autosomal recessive retinitis pigmentosa due to a PDE6A mutation. *Invest Ophthalmol Vis Sci.* 2009;50(2):801–113.
15. Schön C, Pittler SJ, Pittler SJ, et al. Gene therapy successfully delays degeneration in a mouse model of PDE6A-linked retinitis pigmentosa (RP43). *Hum Gene Ther.* 2017;28(12):1180–1188.
16. Sothilingam V, Garrido MG, Jiao K, et al. Retinitis pigmentosa: impact of different *Pde6a* point mutations on the disease phenotype. *Hum Mol Genet.* 2015;24(19):5486–5499.
17. Khateb S, Nassissi M, Bujakowska KM, et al. Longitudinal clinical follow-up and genetic spectrum of patients with rod-cone dystrophy associated with mutations in *PDE6A* and *PDE6B*. *JAMA Ophthalmol.* 2019;137(6):669–679.
18. Khan SY, Ali S, Naeem MA, et al. Splice-site mutations identified in *PDE6A* responsible for retinitis pigmentosa in consanguineous Pakistani families. *Mol Vis.* 2015;21:871–882.
19. Sharon D, Ben-Yosef T, Goldenberg-Cohen N, et al. A nationwide genetic analysis of inherited retinal diseases in Israel as assessed by the Israeli inherited retinal disease consortium (IIRDC). *Hum Mutat.* 2020;41(1):140–149.
20. Dryja TP, Rucinski DE, Chen SH, Berson EL. Frequency of mutations in the gene encoding the alpha subunit of rod cGMP-phosphodiesterase in autosomal recessive retinitis pigmentosa. *Invest Ophthalmol Vis Sci.* 1999;40(8):1859–1865.
21. Schulze-Bonsel K, Feltgen N, Burau H, Hansen L, Bach M. Visual acuities “hand motion” and “counting fingers” can be quantified with the Freiburg visual acuity test. *Invest Ophthalmol Vis Sci.* 2006;47(3):1236–1240.
22. Bowman KJ. A method for quantitative scoring of the Farnsworth Panel D-15. *Acta Ophthalmol (Copenh).* 1982;60(6):907–916.
23. Erb C, Adler M, Stübiger N, Wohlrab M, Zrenner E, Thiel HJ. Colour vision in normal subjects tested by the colour arrangement test ‘Roth 28-hue desaturated’. *Vision Res.* 1998;38(21):3467–3471.
24. Lanthony P. Evaluation of the desaturated Panel D-15. IV. Effect of the repetition of desaturated Panel D-15. *J Fr Ophthalmol.* 1995;18(10):578–583.
25. Vingrys AJ, King-Smith PE. A quantitative scoring technique for panel tests of color vision. *Invest Ophthalmol Vis Sci.* 1988;29(1):50–63.
26. Gould R, Abramson PE, Galasko D, Salmon D. Rate of cognitive change in Alzheimer’s disease: methodological approaches using random effects models. *J Int Neuropsychol Soc.* 2001;7(7):813–824.
27. Nobre JS, da Motta Singer J. Residual analysis for linear mixed models. *Biom J.* 2007;49(6):863–875.
28. Richards S, Aziz N, Bale S, et al. Standards and guidelines for the interpretation of sequence variants: a joint consensus recommendation of the American College of Medical Genetics and Genomics and the Association for Molecular Pathology. *Genet Med.* 2015;17(5):405–424.
29. Wang NK, Mahajan VB, Tsang SH. Therapeutic window for phosphodiesterase 6-related retinitis pigmentosa. *JAMA Ophthalmol.* 2019;137(6):679–680.
30. Cai S, Bressler NM. Aflibercept, bevacizumab or ranibizumab for diabetic macular oedema: recent clinically relevant findings from DRCR.net Protocol T. *Curr Opin Ophthalmol.* 2017;28(6):636–643.
31. Ricci F, Bandello F, Navarra P, Staurengi G, Stumpp M, Zarbin M. Neovascular age-related macular degeneration: therapeutic management and new-upcoming approaches. *Int J Mol Sci.* 2020;21(21):8242.
32. Csaky KG, Richman EA, Ferris FL, 3rd. Report from the NEI/FDA Ophthalmic Clinical Trial Design and Endpoints Symposium. *Invest Ophthalmol Vis Sci.* 2008;49(2):479–489.
33. Berson EL, Sandberg MA, Rosner B, Birch DG, Hanson AH. Natural course of retinitis pigmentosa over a three-year interval. *Am J Ophthalmol.* 1985;99(3):240–251.
34. Birch DG, Anderson JL, Fish GE. Yearly rates of rod and cone functional loss in retinitis pigmentosa and cone-rod dystrophy. *Ophthalmology.* 1999;106(2):258–268.
35. Nagy D, Schönfisch B, Zrenner E, Jägle H. Long-term follow-up of retinitis pigmentosa patients with multifocal electroretinography. *Invest Ophthalmol Vis Sci.* 2008;49(10):4664–4671.
36. Holopigian K, Greenstein V, Seiple W, Carr RE. Rates of change differ among measures of visual function in patients with retinitis pigmentosa. *Ophthalmology.* 1996;103(3):398–405.
37. Kong X, Fujinami K, Strauss RW, et al. Visual acuity change over 24 months and its association with foveal phenotype and genotype in individuals with Stargardt disease: ProgStar Study Report No. 10. *JAMA Ophthalmol.* 2018;136(8):920–928.
38. Corton M, Blanco MJ, Torres M, Sanchez-Salorio M, Carracedo A, Brion M. Identification of a novel mutation in the human PDE6A gene in autosomal recessive retinitis pigmentosa: homology with the *nmf28/nmf28* mice model. *Clin Genet.* 2010;78(5):495–498.
39. Cideciyan AV, Jacobson SG, Roman AJ, et al. Rod function deficit in retained photoreceptors of patients with class B rhodopsin mutations. *Sci Rep.* 2020;10(1):12552.
40. Yang Y, Dunbar H. Clinical perspectives and trends: microperimetry as a trial endpoint in retinal disease. *Ophthalmologica.* 2021;244(5):418–450.

APPENDIX: RD-CURE CONSORTIUM MEMBERS

Members of the RD-CURE Consortium (in institutional and alphabetical order): Centre for Ophthalmology, Eberhard Karls University of Tübingen, Tübingen, Germany: Karl Ulrich Bartz-Schmidt, Sylvia Bolz, M. Dominik Fischer, Susanne Kohl, Laura Kuehlewein, Regine Mühlfriedel, Jonas Neubauer, Alex Ochakovski, François Paquet-Durand, Mathias Seeliger, Vithijanjali Sothilingam, Katarina Stingl, Marius Ueffing, Nicole Weisschuh, Bernd Wissinger, Fabian Wozar, Ahmad Zhou,

Ditta Zobor, and Eberhart Zrenner. Department of Ophthalmology, University Hospital, Ludwig Maximilian University of Munich, Munich, Germany: Stylianos Michalakis. Department of Pharmacy, Center for Drug Research, Ludwig Maximilian University of Munich, Munich, Germany: Martin Biel, Stylianos Michalakis, and Christian Schön. STZ eyetrial at the Centre for Ophthalmology, University

of Tübingen, Tübingen, Germany: Nadine Kahle, Tobias Peters, and Barbara Wilhelm. Department of Ophthalmology, Columbia University, New York, New York: Stephen H. Tsang. Deutsches Zentrum für Neurodegenerative Erkrankungen, Eberhard Karls University of Tübingen, Tübingen, Germany: Christian Johannes Glöckner.